The heart of oxygenic photosynthesis illuminated

Janssen, G.J.

Chapter 2

Observation of the solid-state photo-CIDNP effect in whole cells of cyanobacteria *Synechocystis* sp. PCC 6803

Cyanobacteria, also known as blue green algae, are widely used as model organisms for oxygenic photosynthesis since they represent the simplest photosynthetic organisms containing both PSI and PSII. In this chapter the first photo-CIDNP observed in whole cells of the cyanobacterium *Synechocystis* sp. PCC 6803 is presented. Photo-CIDNP ^{13}C MAS NMR is a powerful tool for understanding the photosynthesis machinery at the cofactor level with atomic selectivity. Combined with selective isotope enrichment, this technique has now opened the door to the study of primary charge separation in whole living cells. This implies that photo-CIDNP MAS NMR studies on oxygenic photosystems are no longer limited to isolated plant photosystems. The results show that the solid-state photo-CIDNP effect is highly conserved in photosynthetic systems as proposed earlier (Matysik *et al.* 2009). In addition, the photo-CIDNP features of PSI and PSII appear to be very similar in plant and cyanobacterial systems, suggesting remarkable conservation of the electronic properties of their photochemical machineries.

The content of this chapter has been published in *Photosynthesis Research* (2010) 104: 275-282

2.1 INTRODUCTION

Natural photosynthesis in plants, algae and several types of bacteria, is initiated by highly efficient light-induced electron transfer, occurring in reaction center (RC) proteins and having a quantum yield close to unity. It has been proposed that this remarkable efficiency is related to the occurrence of correlated radical pairs (Thurnauer and Norris 1980) and the solid-state photo-CIDNP effect (Matysik *et al.* 2009).

Photochemical induced dynamic nuclear polarization (photo-CIDNP) is a well-known phenomenon in liquid NMR (for review see: Hore and Broadhurst 1993; Roth 1996; Goez 1997). It was discovered in 1967 and explained by the radical pair mechanism (RPM) (Bargon and Fischer 1967; Ward and Lawler 1967; Cocivera 1968; Closs and Closs 1969; Kaptein and Oosterhoff 1969). In 1994, Zysmilich and McDermott observed for the first time this new type of photo-CIDNP in frozen and quinone-blocked RCs of purple bacteria *Rb. sphaeroides* R26 by ^{15}N magic-angle spinning NMR (Zysmilich and McDermott 1994). Meanwhile, the exact spin-chemical mechanism of the solid-state photo-CIDNP effect (for reviews see Jeschke 1997; Jeschke and Matysik 2003) in *Rb. sphaeroides* is understood (Daviso *et al.* 2009). Initially, the spin-correlated radical pair is formed in a pure singlet state (Figure 1.8, chapter 1, page 31) and it is, therefore, highly electron correlated. Three mechanisms occur to build up photo-CIDNP under continuous illumination, which run in parallel. In all mechanisms the breaking of the balance of the opposite nuclear spin populations in the two decay branches of the radical pair states leads to *net* steady-state nuclear polarization, which is detected in the NMR experiment: (I) Electron-electron-nuclear three-spin mixing (TSM) breaks the balance of the two radical-pair decay channels by coherent spin evolution within the correlated radical pair state depending of the signs of the electron-electron and of the electron nuclear interactions (Jeschke 1997; 1998). The symmetry breaking is driven by the pseudosecular, off-diagonal, part *B* of the hyperfine interaction. (II) In the differential decay (DD) mechanism (Polenova and McDermott 1999), the symmetry between the two decay channels is broken by the different lifetimes of the states of the correlated radical pair. This means that in the two radical pair spin states different fractions of polarization flow from the electrons to the nuclei. The result is an additional imbalance between the fractions of nuclei in spin-up and spin-down states in the two decay channels. (III) In addition to the two polarization transfer mechanisms TSM and DD, in samples as R26-RCs of *Rb. sphaeroides* having a long lifetime of the triplet donor (^{3}P), a third mechanism may occur that selects nuclear

polarization. In this differential relaxation (DR) mechanism the breaking of antisymmetry of the polarization in the singlet and triplet branch occurs in a non-coherent way. The enhanced relaxation of nuclear spins in the proximity of the high-spin donor partially cancels the nuclear polarization in the donor cofactor. Hence, when the ^{3}P lifetime is comparable to or exceeds the paramagnetically enhanced longitudinal relaxation time, net polarization occurs due to partial extinction of nuclear polarization of the triplet state of the radical pair (Goldstein and Boxer 1987; McDermott *et al.* 1998).

The number of RC species that show the solid-state photo-CIDNP effect is growing. The list contains systems from various bacteria as well as from plants, such as bacterial RCs of *Rb. sphaeroides* WT (Prakash *et al.* 2005) and R26 (Prakash *et al.* 2006), *Rhodopseudomonas acidophila* (Diller *et al.* 2008), *Chlorobium tepidum* (Roy *et al.* 2007) and *Heliobacillus mobilis* (Roy *et al.* 2008) as well as in RCs of plant photosystems I and II (Matysik 2000; Alia *et al.* 2004; Diller *et al.* 2007). It appears that the occurrence of the solid-state photo-CIDNP effect is an intrinsic property of photosynthetic RCs (Roy *et al.* 2008; Matysik *et al.* 2009), although the window of occurrence of this effect is rather limited by kinetic and magnetic parameters (Allen 1968; Jeschke and Matysik 2003). Initially, photo-CIDNP MAS NMR experiments were performed on isolated RCs. Later it became evident that the strong enhancement effect also allows for investigations directly on cells (Prakash *et al.* 2006) or photosynthetic membranes (Roy *et al.* 2008).

In the growing list of natural RCs proven to show the solid-state photo-CIDNP effect, RCs of cyanobacteria remained to be a blank spot. Cyanobacteria are model microorganisms for the study of plant photosynthesis having a photosynthetic apparatus very similar to the one found in plants. In particular, cyanobacterium *Synechocystis* sp. PCC 6803 is of interest, which can grow both autotrophically or heterotrophically in the absence of light and is easily transformed by exogenous DNA. In this chapter we present photo-CIDNP ^{13}C MAS NMR data obtained directly from ^{13}C- isotope labeled whole cells of the cyanobacterium *Synechocystis* sp. PCC 6803.

2.2 MATERIALS AND METHODS

2.2.1 Strains and culture conditions

Wild-type cyanobacterium *Synechocystis* sp. PCC 6803 strain was kindly provided by A.H.M. de Wit of the Biophysics group of Leiden University. Cultures were grown at

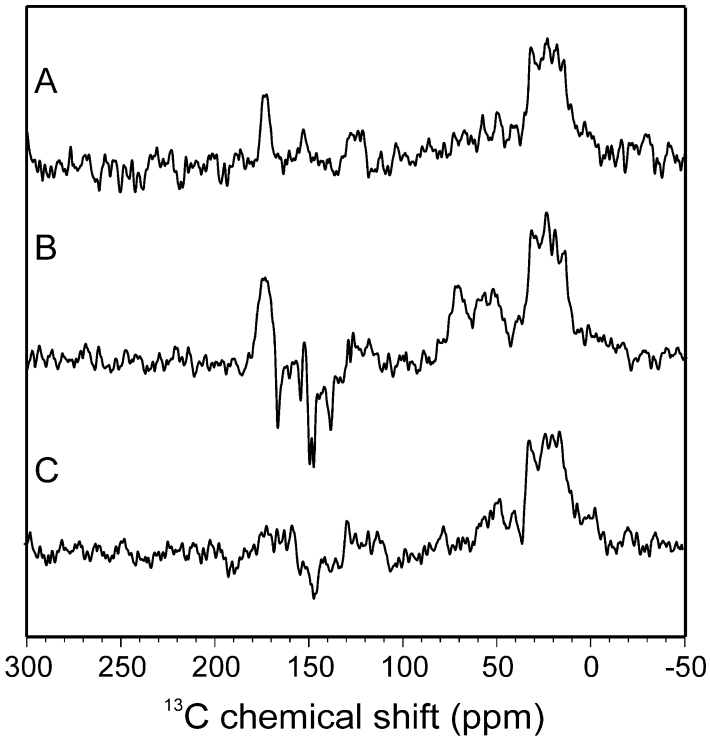

Figure 2.3: ^{13}C MAS NMR spectra of fresh *Synechocystis* sp. PCC 6803 cells obtained in the dark (A), and upon continuous illumination with white light (B). The cells were grown in [4-^{13}C]-ALA supplemented BG-11 medium. Spectrum C shows data obtained by continuous illumination of fresh *Synechocystis* sp. PCC 6803 cells grown in normal BG-11 medium. All spectra have been obtained at a temperature of 235K, in a magnetic field of 4.7 T and with a MAS frequency of 8 kHz.

25°C in standard BG-11 medium (Allen 1968) and illuminated by fluorescent white lamps giving a total intensity of 50 μE $m^{-2}s^{-1}$. Cultures were bubbled with 5% CO_2 enriched air to promote growth. Selective isotope enrichment of chlorophyll (Chl) in *Synechocystis* sp. PCC 6803 was done by growing the cyanobacterium in BG-11 medium supplemented with [4-^{13}C]-δ-aminolevulinic acid (4-ALA) purchased from Cambridge Isotope Laboratories (99% ^{13}C-enriched) to a final concentration of 53 mM.

2.2.2 Determination of the ^{13}C incorporation

Chl *a* was purified from cells grown in 4-ALA supplemented BG-11 medium (labeled sample) and from unlabeled cells (reference sample), according to the following procedure: Cells were harvested by centrifugation for 10 minutes at 13.2 krpm. The cell pellet was resuspended in 1 mL methanol, shaken and centrifuged for 5 min at 2 krpm after which the green supernatant was collected. This procedure was repeated until the pellet showed a white-bluish color. The solvent was evaporated under nitrogen (low light conditions were kept for the entire purification procedure) and the obtained pigments

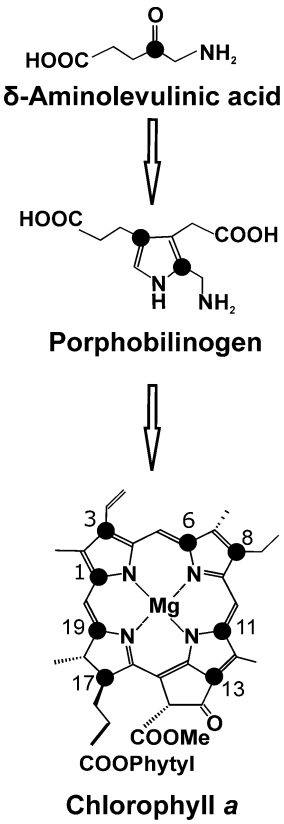

Figure 2.1: Incorporation of [4-^{13}C]-ALA into Chl *a*, black dots indicate the positions of the ^{13}C isotopes

resuspended in 2500 µL running solution, 70:30 (v/v) petroleum ether/acetone. This was loaded on a column filled with silica gel (particle size 40-63 µm, pore diameter ~60 Å) and washed with running solution. Fractions containing pure Chl *a* were identified using a Shimadzu UV-visible spectrophotometer, combined, dried under nitrogen and stored at -20 ˚C.

Mass spectra were measured on a Linear Trap Quadrupole Forier Transform (LTQ–FT) hybrid mass spectrometer (Thermo Fisher Waltham, MA, USA). Spectra were measured in ESI mode, with a source temperature of 200 °C, source voltage of 3.8 kV and tube lens voltage 150V. Chl *a* was dissolved in 90% EtOH and 10% 10 mM ammonium acetate to a final concentration of ~1 mg/mL. The sample was infused with a flow rate of 10 µL/min.

The level of 4-ALA incorporation was determined quantitatively by LC-MS analysis. Chl *a* pigments were extracted from *Synechocystis* cells grown in 4-ALA supplemented BG-11 (labeled sample), and normal BG-11 medium (reference sample). The total level of incorporation (P_{tot}) was determined via an iterative procedure as

described earlier in Schulten *et. al*. (Schulten *et al.* 2002) making use of a weighted sum according to the formula:

$$P_{tot} = \sum_{n=0}^{8} \frac{n}{8} \times P_n \qquad (1)$$

Where n stands for the number of labels present in an isotopomer and P_0 is the corresponding fraction of unlabeled Chl *a* estimated from the isotopic labeling pattern detected from the reference sample (Figure 2.2A). The mass pattern of the unlabeled sample was used to calculate the true intensities (I_t) of the labeled Chl *a*. Thus for example, the true intensity of the n=2 peak at m/z = 895.5 in the labeled Chl *a* spectrum ($^{L}I_t$ (n=2)) was calculated using the true intensities in the labeled spectrum ($^{L}I_t$) and the relative intensities in the unlabeled spectrum ($^{U}I_{\%}$) of the n = 0 and n=1 peaks according to the formula:

$$^{L}I_t(n=2) = {}^{L}I(n=2) - ({}^{U}I_{\%}(n=2) \times {}^{L}I_t(n=0)) - ({}^{U}I_{\%}(n=1) \times {}^{L}I_t(n=1)) \quad (2)$$

Based on the true intensities the Pn could then be calculated according to the formula:

$$P_n = {}^{L}I_t(n) \div \sum_{n=0}^{8} {}^{L}I_t(n) \qquad (3)$$

2.2.3 MAS NMR sample preparation

Selectively isotope enriched *Synechocystis* cells were harvested by centrifugation and washed once with standard BG-11 medium. The pellet was resuspended in a 100 µL of standard BG-11 with low light conditions. The sample was bubbled shortly with nitrogen to remove oxygen and quinone reduced by adding sodium dithionite to a final concentration of 100 mM with oxygen free and near dark conditions. After 30 minutes of incubation in the dark at room temperature (RT) the sample was loaded into an optically transparent 4-mm sapphire MAS rotor under oxygen free conditions. The sample was inserted into the NMR spectrometer right away. The isolated samples of PSI and PSII from spinach at natural abundance have been prepared following the procedures described in refs (Matysik 2000; Alia *et al.* 2004).

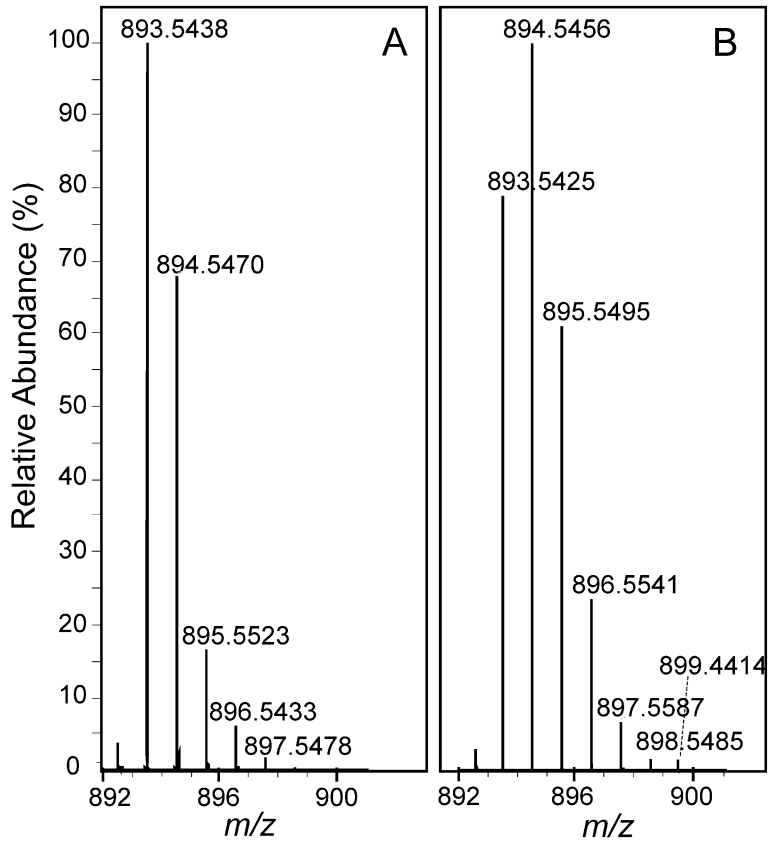

Figure 2.2: Patterns observed with LC-MS spectroscopy around *m/z* = 893 from natural abundance Chl *a* (A) and $^{13}C_{0\text{-}8}$ Chl *a* (B)

2.2.4 Photo-CIDNP MAS NMR experiments

^{13}C-MAS NMR experiments were performed on a DMX-200 NMR spectrometer (Bruker Biospin GmbH, Karlsruhe, Germany). All spectra have been obtained at a sample temperature of 235 K and with a spinning frequency of 8 kHz. The spectra were collected with a spin echo pulse sequence with the CYCLOPS phase cycle of (π/2) pulse under TPPM carbon-proton decoupling. Photo-CIDNP MAS NMR spectra have been obtained under continuous illumination with a 1000-Watt xenon arc lamp.

2.3 RESULTS AND DISCUSSION

2.3.1 Determination of the ^{13}C label incorporation

The biosynthetic route from 4-ALA to Chl *a* is depicted in Figure 2.1. Two molecules of 4-ALA are asymmetrically condensed to form the pyrrole porphobilinogen (PBG). Four molecules of PBG tetramerize, and prior to macrocycle ring closure, the last pyrrole ring is inverted via a spiro-intermediate (Schulten *et al.* 2002). Upon incorporation

of 4-ALA, a maximum of eight ^{13}C can be pairwise incorporated into each Chl *a* molecule, resulting into the specific labeling pattern shown in Figure 2.1 with ^{13}C isotopes incorporated on position C-1/C-3, C-6/C-8, C-11/C-13 and C-17/C-19. Figure 2.2 shows the LC-MS spectra observed in the region of m/z = 893.5 ([M]•+; $C_{55}H_{72}O_5N_4Mg$) from the reference- (A) and the labeled sample (B). Analysis of the isotopic patterns and relative abundances depicted in Figure 2.2 reveal a total incorporation ^{13}C isotope labels (P_{tot}) of 8% (see Table A1 in Appendix A).

2.3.2 Occurrence of the solid-state photo-CIDNP effect in Synechocystis

Spectrum A in Figure 2.3 shows a ^{13}C MAS NMR spectrum of *Synechocystis* cells containing 4-ALA labeled Chl *a* and Phe *a* cofactors obtained in the dark. The spectrum shows, as expected, signals in the aliphatic region between 0 and 50 ppm, in the aromatic region as well as in the region of the amide carbonyls. Probably some of the aromatic ^{13}C response is due to the isotope labelling. Upon illumination with continuous white light (spectrum 2.3B), additional signals occur between 170 and 120 ppm that are predominantly emissive (negative). It is also possible that light-induced signals occur in the aliphatic region between 50-80 ppm, obscured by overlap with dark signals and a high noise level.

Spectrum C in Figure 2.3 shows a ^{13}C MAS NMR spectrum of another preparation of *Synechocystis* cells with ^{13}C at natural abundance, obtained with continuous illumination. In these conditions, it is difficult to identify light-induced signals, although there may be some weakly emissive signal at ~150 ppm chemical shift.

Until now, in two other whole cell systems, for the purple bacterium *Rb. sphaeroides* R26 (Prakash *et al.* 2006; Thamarath *et al.* 2012) and for *Heliobacillus* (*Hb*.) *mobilis* (Thamarath *et al.* 2012) the observation of the solid-state photo-CIDNP effect has been reported. However, for those systems, only one type of RC is present and no isotope labelling was required. Here we show that the solid-state photo-CIDNP effect can also be observed in intact cyanobacterial cells containing both PSI and PSII. In order to recognise the light-induced signals in *Synechocystis*, however, specific isotope labelling was necessary. The necessity to use labels for *Synechocystis* suggests that the intensity of the light-induced signals is about of a factor of 30 weaker than for RCs of *Rb. sphaeroides* R26. Assuming that the solid-state photo-CIDNP mechanisms are similar across species

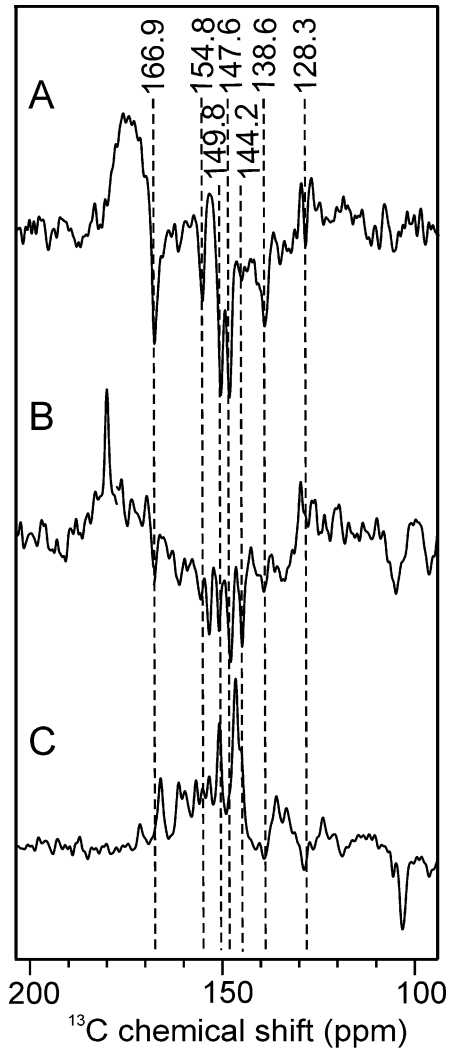

Figure 2.4: (A) Aromatic and carbonyl regions of the ^{13}C MAS NMR photo-CIDNP data collected from fresh [4-^{13}C]-ALA labeled *Synechocystis* sp. PCC 6803 cells shown in Figure 4A are reproduced in the upper trace. The two lower traces show the corresponding ^{13}C regions from photo-CIDNP spectra collected,from isolated PSI (B) and PSII (C) particles from spinach containing ^{13}C at natural abundance. MAS centerband assignments are indicated with vertical dashed lines. The spectra were obtained by continuous illumination with white light at a temperature of 235 K, in a magnetic field of 4.7 Tesla and with a MAS frequency of 8 kHz

and protein complexes, the weak intensity for *Synechocystis* sp. PCC 6803 may be due to (i) incomplete reduction of the acceptor site, (ii) lower concentration of the photosystems caused by the presence of other cellular units, or (iii) destructive interference of photo-CIDNP signals from PSI and PSII.

2.3.3 Assignment of light-induced signals

Trace A in Figure 2.4 shows the aromatic and carbonyl regions of spectrum 2.3B. The light-induced signals are indicated with dashed lines and originate from the 4-ALA labeled Chl *a* and Phe *a* cofactors. Table 2.1 shows the chemical shifts of the observed

Table 2.1: ^{13}C chemical shifts of the photo-CIDNP signals obtained at 4.7 T compared with data from the literature. Abbreviations: σ = chemical shift, a = absorptive signal, e = emissive signal.

Chemical shifts				
Chl *a*	assignment (tentative)	PSI	PSII	PSI+PSII
σ_{ss} [a]		σ [b]	σ [c]	σ [d]
170.0	19	167.1 e	166.8 a	166.9 e
162.0	14	160.4 e	162.2 a	
155.9	1	154.8 e	156.0 a	154.8 e
154.4	6		154.3 a	149.8 e
154.0	16	152.6 e	151.6 a	
150.7	4	149.9 e	149.2 a	
147.2	11	147.2 e	147.7 a	147.6 e
147.2	9			
146.2	8	144.2 e	146.0 a	144.2 e
138.0	3	138.6 e	137.4 a	138.6 e
136.1	2	~136 e	136.0 a	
134.0	12		133.9 a	
133.4	7	~ 132 e	~ 132.0 a	
126.2	13			128.3 e
108.2	10	105.4 e	106.9 e	~104.5 e
102.8	15		104.7 e	
98.1	5		97.9 e	
93.3	20		92.2 e	
51.4	17			

[a] (Schulten *et al.* 2002), data obtained from solid aggregates of Chl *a*.
[b] (Alia *et al.* 2004), data obtained from isolated PSI particles from spinach.
[c] (Diller *et al.* 2007), data obtained from D1D2 particles of spinach.
[d] This work, data obtained from whole cells *Synechocystis* sp. PCC 6803.

signals and summarizes literature values for Chl *a* aggregates and light-induced signals for isolated PSI and D1D2 particles (Boender *et al.* 1995; Alia *et al.* 2004; Diller *et al.* 2005). With the possible exception of the absorptive feature at 153.4 ppm (see below), all light induced signals are of emissive nature.

As suggested by Table 2.1, most of the light-induced signals observed in *Synechocystis* sp. PCC 6803 cells appear at frequencies matching very well with those observed in isolated photosystems of spinach. For example, the signals at 166.9, 154.8, 147.6, 144.2 and 138.6 ppm are observed in isolated PSI at very similar frequencies. This similarity suggests that photosystems are highly conserved even between different families. We also conclude that the isolation of the photosystems from plants does not significantly affect

the electronic properties of the photochemical machinery. Spectra B and C in Figure 2.4 show ^{13}C photo-CIDNP MAS NMR data obtained from isolated PSI and PSII obtained

from spinach with ^{13}C at natural abundance. The spectrum of PSI is entirely emissive in the aromatic region (spectrum B). In contrast, the spectrum of PSII shows in the region from 180 to 130 ppm only absorptive signals (spectrum C). Hence, most probably all emissive signals in spectrum 2.4A arise from PSI. Three possible reasons may explain the absence of PSII resonances: (i) The PSI/PSII ratio in *Synechocystis* sp. PCC 6803 is known to be strongly in favour of PSI with PSII being up to 9 times less abundant (Rögner *et al.* 1990), (ii) PSII proteins may degrade following intense illumination, (iii) If the chemical shifts of the signals from PSI and PSII are very similar at the isotope labeled positions (cf. Table 2.1), absorptive PSII signals may be cancelled by dominant emissive PSI signals. The emissive photo-CIDNP signals in the aromatic region can thus be attributed to the specifically isotope labeled carbons C-1, C-3, C-6, C-8, C-11, C-13, and C-19 (Figure 2.1) of PSI.

Two absorptive signals may be light-induced, at ~170 and 153.4 ppm (spectrum 2.4B). At these positions positive signals can arise from PSII that are not cancelled by emissive PSI signals (see spectrum 2.4C). In addition, two broad absorptive resonances occur with maxima around 70 and 50 ppm in spectrum 2.4B. During continuous illumination of selectively enriched RCs, labeled aliphatic carbons may gain intensity indirectly by spin diffusion from labeled aromatic carbons nearby which can explain the origin of the enhanced aliphatic response in spectrum 2.4B (Matysik *et al*. 2001). A possible explanation may be that these positive light-induced signals indeed originate from PSII, while the light-induced signals in the aromatic region originate from PSI. In that case, the PSII signal would be suppressed in the aromatic region and dominate the aliphatic region due to different relaxation properties. This would imply an almost complete destructive interference of PSI and PSII signals. Investigations on systems with a different ratio between PSI and PSII may provide further insight.

2.3.4 Activity of sample upon storage

Photo-CIDNP signals have been observed exclusively in samples prepared from *freshly* harvested cells. Samples prepared from previously frozen 4-ALA labeled cells, which were otherwise treated identically, did not show the solid-state photo-CIDNP effect (data not shown). Likewise, samples prepared from freshly harvested cells quickly lost activity upon storage at -20^{o}C, to about 70% of the photo-CIDNP intensity after two

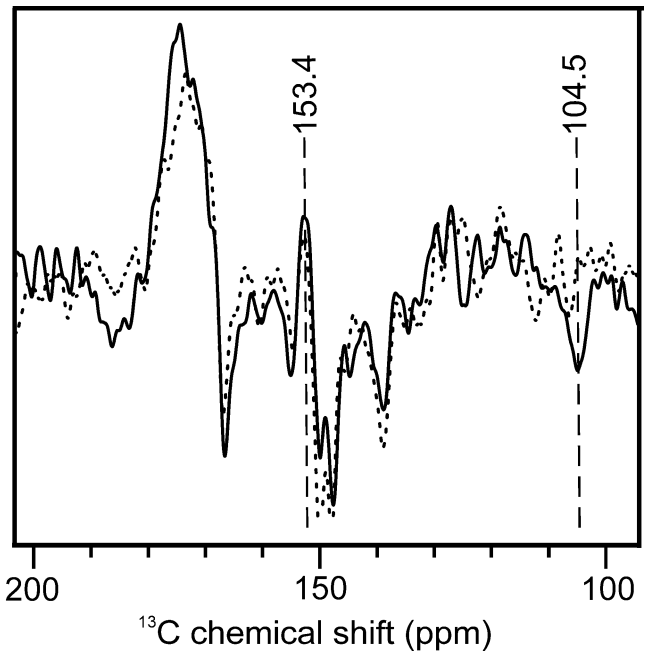

Figure 2.5: ^{13}C MAS NMR spectra of fresh [4-^{13}C]-ALA labeled *Synechocystis* cells obtained by continuous illumination with white light from hour 0 to 25 (solid trace) and hour 50 to 75 (dashed trace). The 104.5 and 153.4 ppm centerbands are visualized by dashed lines.

weeks of storage. In contrast, samples of isolated PSI or D1D2-PSII particles of spinach (Alia *et al.* 2004; Diller *et al.* 2005) did not show a significant loss of activity after storage at -20 ˚C for up to several years.

2.3.5 Light-induced changes in the sample

Using a freshly harvested sample, signals started to appear after 12 hours of measurement. In contrast, in a sample already exposed for 50 hours to white light before, photo-CIDNP signals arose after 4 hours (data not shown). Figure 2.5 shows the aromatic region of two ^{13}C MAS NMR spectra collected from fresh 4-ALA labeled *Synechocystis* sp. PCC 6803 cells obtained under continuous illumination with white light from hour 0 to 25 (solid line) and hour 50 to 75 (dashed line). It seems that signals that can be considered characteristic for PSII (spectrum 2.4C), diminish upon extended illumination. In particular the positive features at 170 and 153.4 ppm, as well as the emissive signal at 104.5 ppm are significantly weakened in the second data set.

A possible explanation could rely on the fact that PSI is, compared to PSII, known to be very difficult to reduce (Feldman *et al.* 2007) and its reduction might be ongoing during the measurement at 235K. This is in agreement with the observation that upon

decreasing the incubation time after reduction with sodium dithionite from 30 to 10 minutes, the emissive signals assigned to PSI are weakened significantly. It may be that the absorptive resonances of more efficiently reduced PSII initially slow down the build-up of emissive PSI signals while upon full reduction of PSI the PSII signals, having opposite signs with respect to the PSI signals, are fully cancelled. This is consistent with the fact that the PSI/PSII ratio in *Synechocystis* sp. PCC 6803 is known to be strongly in favour of PSI (Rögner *et al.* 1990). In addition, since PSI is much more robust than PSII after several hours of illumination PSII may be degraded (Mattoo *et al.* 1984), allowing for a faster build-up of PSI signals. Indeed the typical marker of the PSII spectrum, the emissive signal at ~104.5 ppm, diminishes upon prolonged illumination while the PSI signals remain.

2.3.6 Summary and Conclusion

The occurence of the solid-state photo-CIDNP effect, which appears to be highly conserved in photosynthetic systems, has been demonstrated in cyanobacteria. In addition, the photo-CIDNP features of PSI and PSII appear to be similar in plant and cyanobacterial systems, suggesting conservation of the electronic properties of their photochemical machineries. The occurrence of the effect also in cyanobacterial photosystems directly in prokaryotic cells demonstrates that photo-CIDNP MAS NMR studies on oxygenic photosystems are not limited to isolated photosystems from higher plants but can also be conducted on whole cells. This opens the possibility to apply this method in the analysis of systems in which a further isolation has not yet been established or is too expensive.